

Vibrational Analysis of Manganese(II) Oxalates Hydrates: An In Silico Statistical Approach

Haruna L. Barazorda-Ccahuana, Miroslava Nedyalkova,* Ilija Kichev, Sergio Madurga, Borjana Donkova, and Vasil Simeonov

Cite This: *ACS Omega* 2020, 5, 9071–9077

Read Online

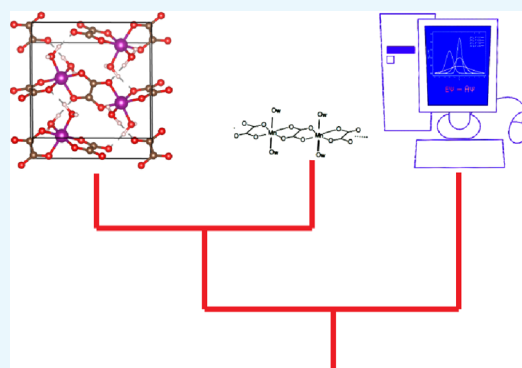
ACCESS |

Metrics & More

Article Recommendations

Supporting Information

ABSTRACT: The experimental and computational vibrational study for three different manganese(II) oxalates hydrates was explored. The elucidation of IR and Raman spectra were discussed based on their structural singularity; in the same way, they establish some interesting relations between them in the field of computational and statistical approaches. The density functional theory (DFT) computational approach was conducted for accurate prediction and interpretation of the intermolecular effects based on experimental and calculated IR and Raman spectra in the solid-state data in combination with multivariate statistical technique. The proposed computational scheme was also explored for the case of the isolated-molecule model. The goals of the study were to access the accuracy of the proposed procedure for solid-state calculations along with electron calculations for the isolated molecules and to reveal the similarities within the groups of objects by the cluster analysis (CA) techniques and two-way CA for the data. The presented simulation procedure should be very valuable for exploring and to classify other oxalate compounds.



INTRODUCTION

The vibrational spectroscopy is a powerful tool for the characterization of molecules and chemical reactions. In the past years, this method has been useful to study many oxalates widely distributed in nonliving and living organisms. The calculation of vibrational spectra, optical, and elastic properties for the crystals has recognized to be a difficult task. All of these are highly correlated with the structural parameters. Thus, obtaining the accurate spectra, for example, would require the know-how of appropriated coordinates and cell parameters.

Currently, the simplest form of oxalate (C_2O_4) dicarboxylate is a typical transition metal oxide precursor that develops a strong variety of salts and metallic complexes.^{1–4} The oxalate anions can be coordinated to metallic atoms through oxygen atom, increasing their electrochemical properties.⁵ Our focus is on the three forms of manganese(II) oxalate: monoclinic α - $MnC_2O_4 \cdot 2H_2O$ (SG $C2/c$),⁶ orthorhombic γ - $MnC_2O_4 \cdot 2H_2O$ (SG $P2_12_12_1$),⁷ and orthorhombic $MnC_2O_4 \cdot 3H_2O$ (SG $Pcca$).⁸ The prescriptions for their preparation from aqueous solutions, containing Mn^{2+} and $C_2O_4^{2-}$ ions, were given by Huizing.⁹ The main differences in their structure were commented by Mancilla et al.¹⁰ based on a thorough vibrational spectroscopic investigation.

The main goal of this work is to transfer a valuable and proven approach based on solid-state quantum chemical calculation for prediction of vibrational spectra of oxalate crystals. Multivariate statistical interpretation of infrared (IR)

and Raman spectral data (hierarchical cluster analysis) have been used to determine specific structural conditions derived from the procedure of synthesis giving different final compounds. In addition, the accuracy of the obtained properties usually also depend of the computational used methods. In the last decay, the increasing of powerful computational methods and the presence of more advance and sophisticated quantum-mechanical approximations, first-principles approaches based on density functional theory (DFT) can now be used to model an appropriately large variety of molecular crystals.

Furthermore, we yield light on the performance and accuracy of the modern quantum-chemical models to predict vibrational spectra of metal oxalates and to show cheaper computational alternatives using single-molecule calculations.¹¹ Additionally, multivariate statistical analysis of IR and Raman spectral data (hierarchical cluster analysis, two-way clustering) was used to determine the similarities among oxalates and among their vibration bands.^{12,13} Cluster analysis of analytical

Received: October 15, 2019

Accepted: March 10, 2020

Published: April 15, 2020



Table 1. Wavenumbers (in cm^{-1}) and Assignment of the Vibrational Spectra of the Three Manganese(II) Oxalates Hydrates in the Isolated and Crystal Form

objects	labels	experimental		calculated freq.		calculated freq. ^a	
		IR	Raman	IR	Raman	IR	Raman
$\alpha\text{-MnC}_2\text{O}_4\cdot 2\text{H}_2\text{O}_\nu$ (C–O)	C1	1625	1625	1550	1548	1420	1524
$\alpha\text{-MnC}_2\text{O}_4\cdot 2\text{H}_2\text{O}_\nu$ (C–O)	C2	1362	1465	1320	1398	1300	1310
$\alpha\text{-MnC}_2\text{O}_4\cdot 2\text{H}_2\text{O}_\delta$ (O–C–O)	C3	815	855	798	815	750	825
$\gamma\text{-MnC}_2\text{O}_4\cdot 2\text{H}_2\text{O}_\nu$ (C–O)	C4	1640	1641	1603	1629	1558	1639
$\gamma\text{-MnC}_2\text{O}_4\cdot 2\text{H}_2\text{O}_\nu$ (C–O)	C5	1460	1492	1452	1469	1401	1455
$\gamma\text{-MnC}_2\text{O}_4\cdot 2\text{H}_2\text{O}_\nu$ (C–O)	C6	1353	1462	1350	1458	1325	1444
$\text{MnC}_2\text{O}_4\cdot 3\text{H}_2\text{O}_\nu$ (C–O)	C7	1605	1614	1599	1587	1504	1568
$\text{MnC}_2\text{O}_4\cdot 3\text{H}_2\text{O}_\nu$ (C–O)	C8	1372	1478	1368	1468	1352	1455
$\text{MnC}_2\text{O}_4\cdot 3\text{H}_2\text{O}_\nu$ (C–O)	C9	811	913	850	822	855	802
$\alpha\text{-MnC}_2\text{O}_4\cdot 2\text{H}_2\text{O}_\rho$ (H_2O) + δ ring	C10	604	579	685	685	651	574
$\gamma\text{-MnC}_2\text{O}_4\cdot 2\text{H}_2\text{O}_\rho$ (H_2O) + δ ring	C11	697	612	582	541	524	514
$\alpha\text{-MnC}_2\text{O}_4\cdot 2\text{H}_2\text{O}_\nu$ (Mn–O)	C12		517	500	487	471	452
$\gamma\text{-MnC}_2\text{O}_4\cdot 2\text{H}_2\text{O}_\nu$ (Mn–O)	C13	550		523	538	518	512
$\text{MnC}_2\text{O}_4\cdot 3\text{H}_2\text{O}_\nu$ (Mn–O)	C14	555	515	535	500	485	477

^aIsolated molecule.

data is routinely applied to identify groups of similarity, which can be reliably interpreted.^{14–18}

RESULTS AND DISCUSSION

Experimental XRD, IR, and Raman Spectra. The experimental values of IR and Raman spectra from manganese(II) oxalates hydrates are compared with the theoretical spectra obtained with the isolated molecule and with the crystal forms (Table 1).

The equilibrium geometries obtained for the crystal and isolated forms are depicted in Figure 1. The combination of experimental vibrational spectra with the predicted theoretically of these oxalates in a statistical study could be interesting to have a better knowledge of the relation of the structural properties with the vibrational properties.

X-ray Crystallographic and Optimized Structures. In Figure 2, it can be seen the comparison of XRD results. A very good matching between calculated and theoretical diffractograms is observed. It can be seen in Figure 2a, that the double peak around 19 degrees is also reproduced in the calculations. In Figure 2b,c, the strongest reflections are those simulated at 16 and 14 degrees, respectively. These peaks are also very well reproduced by the calculations. With respect to the peaks with less intensity, a good correspondence is also obtained.

Cluster Analysis. The data set subject to hierarchical cluster analysis had a dimension of 15 objects and 6 variables [15×6], where the objects of the study were three manganese oxalates systems (spectral data obtained by experimental and computational approaches). The variables are IR and Raman frequencies, which describe different composites. A measure of similarity was obtained with Ward's method linkage using squared Euclidean distances. The values of 1/3 and 2/3Dmax of Sneath's index were used to determine cluster significance.

In Figure 3, the dendrogram shows that the analytical values were classified into three primary groups and were associated at different levels of similarity. A clear difference exists between the three branches of the dendrogram, which indicates a high level of dissimilarity. Two clusters could be identified; one cluster is composed by the IR calculated using the crystal structures or the isolated molecules. The other cluster is composed by the Raman frequencies calculated using the crystal structures and the isolated molecules. At higher

dissimilarity, there are the IR and Raman spectra, which are experimentally obtained.

In the IR calculated cluster, the matching of the data is obtained, although different structure forms, crystal and isolated, are used. The combined characterization of IR spectroscopy complemented by DFT calculations allowed us to propose a paradigm for the full identification of general manganese. The pattern of the two techniques denotes therefore a very effective tool for the characterization of different manganese oxalates complexes.

The same behavior is observed in the calculated Raman clusters, which collect the calculated Raman for the crystal and the isolated molecules. With the information obtained for the similarities pattern in the both clusters, we demonstrate a robust, computational workflow for using the isolated molecules instead of periodic calculations using crystal structures. By the obtained results, we probe the adequate performance of modern DFT appropriate methods in the spectroscopy field, at least in the context of the kind of the studied compounds. Notably, a good linear correlation between the IR and Raman vibrational spectrum was obtained for the case of crystal forms and isolated molecules, as shown in Figure S1 (Supporting Information). However, the best prediction is obtained in the calculations that use crystal forms as the best mean absolute error (MAE) and mean square error (MSE) values were obtained in the prediction of IR and RAMAN bands using these crystal structures (Table S5).

In the dendrogram of IR and Raman frequencies, two clusters are identified (Figure 4). The first cluster shows the relationship among the high frequency vibrational bands. These are especially remarkable, taking into account the structures differences for the hydrates presented. The observed linkage in the spectroscopic vibrations clearly supports the conclusion that also in the trihydrate complex, the Mn(II) coordination must be comparable to the other two hydrates. Moreover, it is quite difficult to discriminate the three compounds based on the spectral analysis in this observed spectral range. The second cluster indicates the similarity between the objects in the range of the low frequencies.

In order to better understand the relationship between cases and variables (spectral characteristics), the two-way clustering approach was applied. It makes possible to illustrate the link

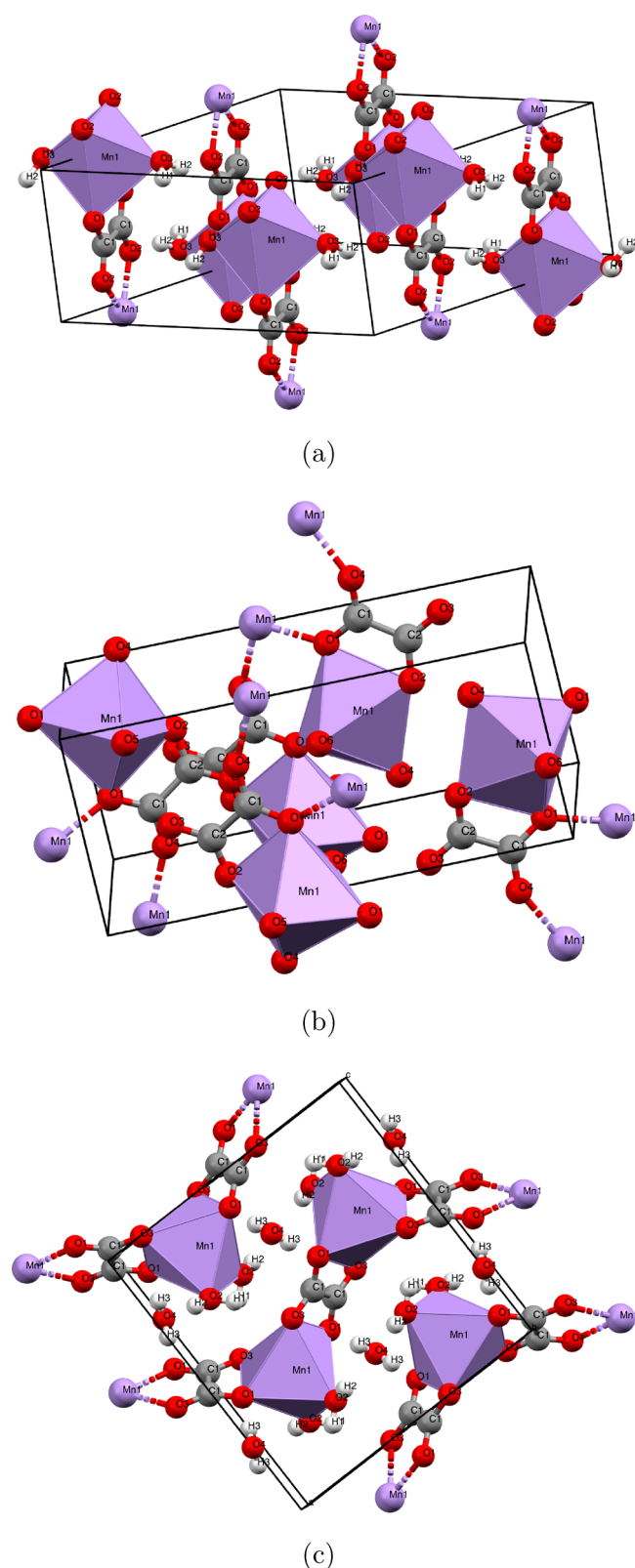


Figure 1. Molecular structure of Mn(II) oxalates hydrates. (a) α - $\text{MnC}_2\text{O}_4 \cdot 2\text{H}_2\text{O}$, (b) γ - $\text{MnC}_2\text{O}_4 \cdot 2\text{H}_2\text{O}$, and (c) $\text{MnC}_2\text{O}_4 \cdot 3\text{H}_2\text{O}$.

between the clusters of cases with the clusters of variables. In such a way, the discriminant parameters for each cluster could be found.

The two-way clustering of Pearson's correlation (P) coefficients among experimental and calculated vibrations

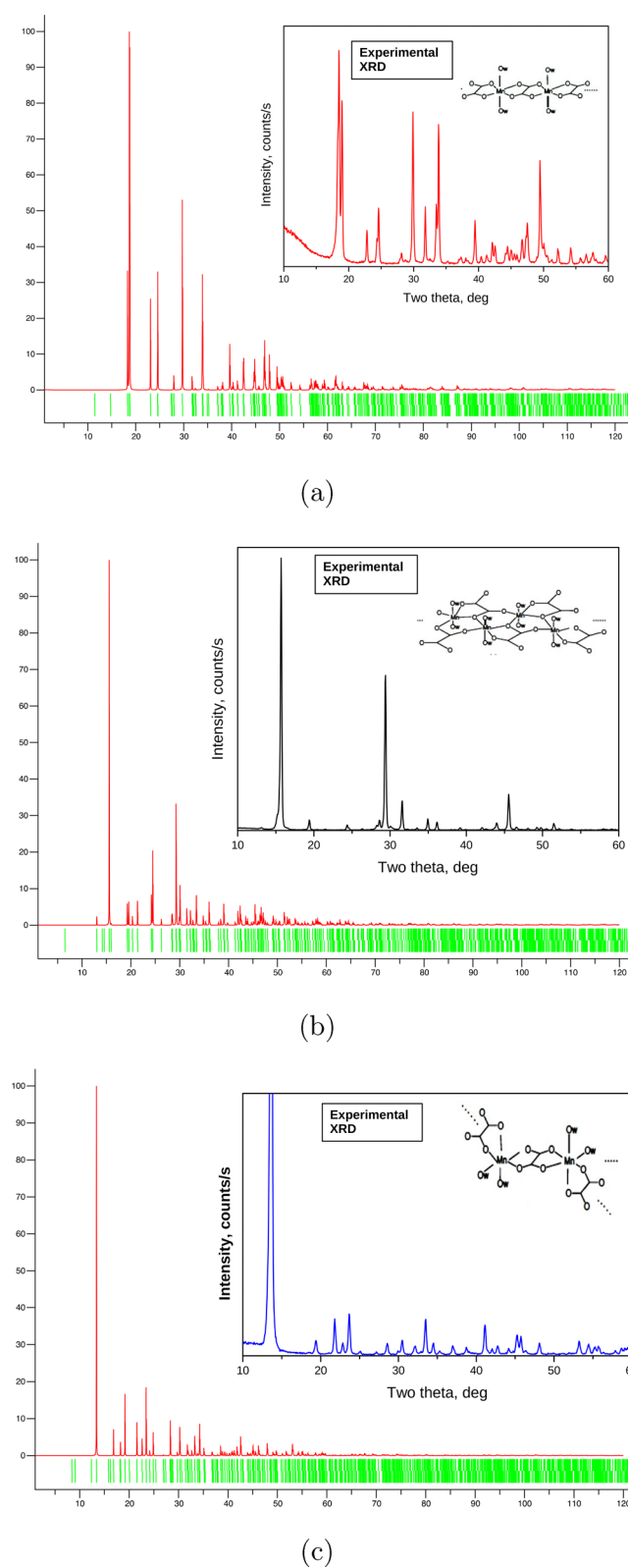


Figure 2. Computed and experimental (inset) of XRD. (a) α - $\text{MnC}_2\text{O}_4 \cdot 2\text{H}_2\text{O}$, (b) γ - $\text{MnC}_2\text{O}_4 \cdot 2\text{H}_2\text{O}$, and (c) $\text{MnC}_2\text{O}_4 \cdot 3\text{H}_2\text{O}$.

with different manganese(II) oxalates hydrates revealed distinct patterns (Figures S1 and S2). It can be seen in Figure 5 that three different groups could be distinguished. The main reason for separation of the manganese oxalates samples into three classes is because of different vibrational spectra. The

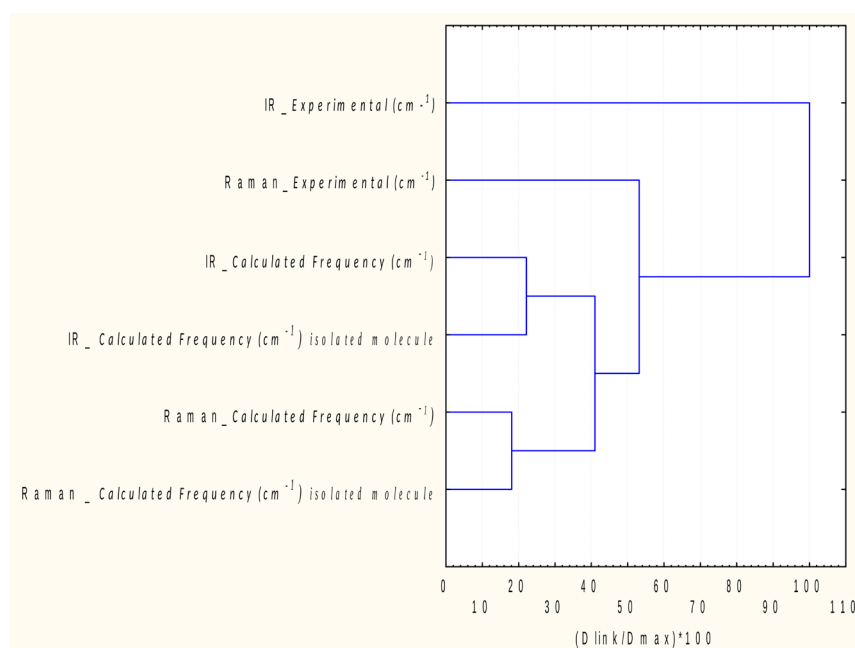


Figure 3. Dendrogram of the experimental and IR and Raman frequencies computational methods obtained using squared Euclidean distance and Ward's method.

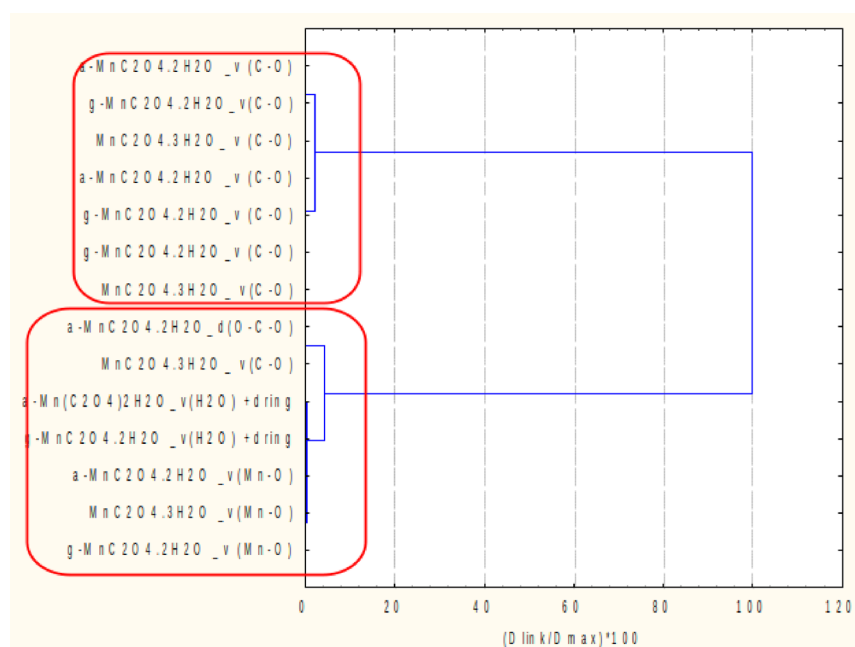


Figure 4. Dendrogram of IR and Raman frequencies of the three Mn(II) oxalates hydrates.

class with the highest P coefficients corresponds to high vibrations, mainly to the ν (C–O) assignments. The second class with intermediate P values corresponds to intermediate vibrations. Finally, the last class corresponds to those vibrations with the lowest frequencies.

CONCLUSIONS

First-principles methods applied to model vibrational properties in an accurate and well-adjusted fashion will make these methods appropriate for prediction and analysis of different molecular crystals in the future. Vibrational spectroscopy and in particular Raman spectroscopy constitute important properties that could be analyzed with the combination of ab initio

and cluster analysis. In the present study, a comprehensive analysis of the IR and Raman spectra of the three known manganese(II) oxalates hydrates was performed, contributing valuable information for the easy characterization of these species. DFT calculations were performed with crystal and isolated molecules of three manganese(II) oxalate hydrates.

The comparison was performed with the experiments that were performed with samples in the crystal state. Based on the obtained results, there are small differences between theoretical and measured vibrational frequencies. Cluster analysis confirms the existence of a strong pattern between the crystal and isolated form for the three manganese compounds. The linear regression between the theoretical frequencies for the crystal

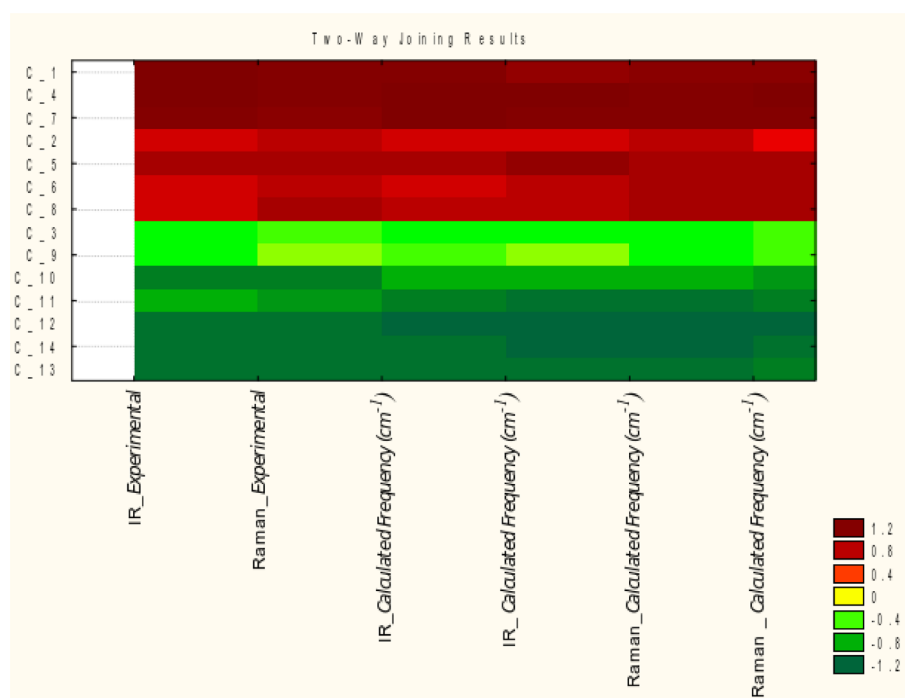


Figure 5. Heat map constructed by the two-way clustering of Pearson's correlation coefficients.

form and isolated ones confirms the accuracy of the applied computational protocol.

In conclusion, the cluster analysis provides an effective way for structure data interpretation and assessment of the structural relationship between hydrates. The clustering reveals new perspectives of interpretation of results by creating groups of similarity between the compounds, which could serve as “fingerprints” for a particular type of oxalate-containing compounds.

MATERIALS AND METHODS

The spectroscopic data are obtained by a synthetic procedure and spectroscopic measurements described by Mancilla et al.,¹⁰ whereas the experimental XRD data of the three manganese(II) oxalates were measured. The detailed description of computational methods used to obtain the relaxed structures, vibration properties, and chemometrics techniques for clustering analysis is given below. We have used the experimental XRD data of manganese(II) oxalates hydrates and VESTA software database to determine basic atomic coordinates of all atoms of the three compounds. We applied a quantum approach to obtain the electronic structure of atoms based on density functional theory (DFT).^{19–21} The DFT optimized structural parameters were compared with experimental XRD crystallographic data. The most stable geometrical optimized structure was used for theoretical calculations.

Computational Spectroscopy Using Gaussian. The molecular structures of the title molecules in the ground state (isolated state) were optimized using DFT/B3LYP with 6-311++G(d,p) basis set level. In this case, this type of functional and base set was based on the optimal results work of 3d transition metals.^{22–24} Then, the calculated optimized structures were used in the vibrational frequency calculations. The calculated harmonic vibrational frequencies have been

scaled by 0.9614 for all systems.²⁵ The Gaussian 09 program package was used in these calculations.²⁶

Computational Spectroscopy Using Quantum Espresso. The periodic structures were calculated with ultrasoft pseudopotentials (USPP) and a plane-wave (PW), implemented in the Quantum Espresso (QE) integrated suite of computer codes.²⁷ The local density approximation (LDA) with Perdew, Burke, and Ernzerhof (PBE) was applied as it allows computing large systems with sufficient accuracy at a limited computation cost. Every k-point in the wave functions was represented by the numerical coefficients of a finite set of plane waves, determined by a kinetic energy cut-off. The k-points were generated automatically, following the Monkhorst–Pack (MP) scheme.²⁸ QE is one of the most many popular computational materials software packages to apply the MP scheme for generating k-points. In the discussed scheme, the k-point grids are regular and aligned with the reciprocal lattice vectors. There exists a mapping between each regular k-point grid and a real-space superlattice that defines the Born–von Karman boundary conditions for the periodicity of the wave functions. Interatomic forces were computed in the frame of Hellmann–Feynman theorem.²⁹

The Qe package, based on a PW basis (40 Ry in all calculations) was used. The atomic positions were fully relaxed until the residual forces on each atom were less than 10⁻⁵ Rydberg/bohr. Starting from the relaxed position, the molecular vibrational modes, plus their infrared intensities and non-resonant-Raman cross-sections, using the density functional perturbation theory were computed.

Cluster Analysis. Cluster analysis (CA) is eminent and commonly used in data mining approach with its hierarchical and non-hierarchical algorithms.^{30,31} The defined objects could be distinguished by a set of variables, and by the application of cluster analysis, the similarity pattern could be revealed. The first step of data scaling (auto-scaling or z-transform) is to normalize dimensionless numbers to replace the real data

values necessary. Thus, large differences in absolute values could be reduced to small differences in normalized data. The comparison between the objects (or more strictly, the distance) in the variable space has to be determined. Very often, Euclidean's distance is used for clustering determination. The correlation coefficient calculations between the objects are the different approaches for measuring the similarity. Thus, from the input data matrix (raw data), a similarity matrix could be constructed. Nowadays, a wide variability of hierarchical algorithms of object linkage include the single linkage, the complete linkage, and the average linkage methods. In this study, Ward's linkage method was used. The representation of the results of the cluster analysis is performed as a tree scheme called dendrogram comprising a hierarchical clustering.

Two-Way Clustering. The research question in tree clustering is how to link similar objects in similarity groups or clusters. However, all tasks in multivariate statistics are related to cases (observations) and/or variables describing the objects. It turns out that the clustering of both may yield useful results. For example, imagine a study where a medical researcher has gathered data on different measures of physical fitness (variables) for a sample of heart patients (cases). The researcher may want to cluster cases (patients) to detect clusters of patients with similar syndromes. At the same time, the researcher may want to cluster variables to detect clusters of measures that appear to tap similar physical abilities. In the two-way clustering or joining, one can choose to cluster cases and variables simultaneously. Two-way joining is useful in (the relatively rare) circumstances when one expects that both cases and variables will simultaneously contribute to the uncovering of meaningful patterns of clusters. For example, returning to the example above, the medical researcher may want to identify clusters of patients that are similar with regard to particular clusters of similar measures of physical fitness. The difficulty with interpreting these results may arise from the fact that the similarities between different clusters may pertain to (or be caused by) somewhat different subsets of variables. In the cluster analysis, assessing the number of clusters and proving information for the density of population of data that are clustered are not actually homogeneous. However, the two-way connection method of clustering decreases the inhomogeneity in both by the clustering of cases and in variables. The two-way joining offers a powerful exploratory data analysis tool. One major advantage of the method (which resembles correspondence analysis) is the option to explain the specificity of formation clusters of cases by certain groups of variable and, vice versa, to related clustering of variables to sets of cases (objects).

■ ASSOCIATED CONTENT

SI Supporting Information

The Supporting Information is available free of charge at <https://pubs.acs.org/doi/10.1021/acsomega.9b03434>.

(Figures S1 and S2) The Pearson's correlation coefficients plots, (Table S1) the experimental data of three manganese(II) oxalates hydrates, (Table S2) the predicted intensities for IR, (Tables S3–S8) the bond length, bond angle, and torsion angle for α - $\text{MnC}_2\text{O}_4 \cdot 2\text{H}_2\text{O}$, γ - $\text{MnC}_2\text{O}_4 \cdot 2\text{H}_2\text{O}$, and $\text{MnC}_2\text{O}_4 \cdot 3\text{H}_2\text{O}$, and (Table S9) the mean absolute error (MAE) and mean square error (MSE) descriptors (PDF)

■ AUTHOR INFORMATION

Corresponding Author

Miroslava Nedyalkova – Department of Inorganic Chemistry, Faculty of Chemistry and Pharmacy, University of Sofia St. Kl. Okhridski, 1164 Sofia, Bulgaria; orcid.org/0000-0003-0793-3340; Email: mici345@yahoo.com

Authors

Haruna L. Barazorda-Ccahuana – Centro de Investigación en Ingeniería Molecular-CIIM, Vicerrectorado de Investigación, Universidad Católica de Santa María, 04000 Arequipa, Peru; orcid.org/0000-0001-8791-0506

Ilia Kichev – Department of Inorganic Chemistry, Faculty of Chemistry and Pharmacy, University of Sofia St. Kl. Okhridski, 1164 Sofia, Bulgaria

Sergio Madurga – Materials Science and Physical Chemistry Department and IQTCUB, Universitat de Barcelona, 08028 Barcelona, Spain; orcid.org/0000-0002-8135-7057

Borjana Donkova – Department of Inorganic Chemistry, Faculty of Chemistry and Pharmacy, University of Sofia St. Kl. Okhridski, 1164 Sofia, Bulgaria

Vasil Simeonov – Department of Analytical Chemistry, Faculty of Chemistry and Pharmacy, University of Sofia St. Kl. Okhridski, 1164 Sofia, Bulgaria

Complete contact information is available at: <https://pubs.acs.org/10.1021/acsomega.9b03434>

Notes

The authors declare no competing financial interest.

■ ACKNOWLEDGMENTS

NIS-SU projects found, grant number 80-10-152/16.04.2019 funded by the Sofia University. The author M.N. is grateful for the additional support by the project "Information and Communication Technologies for a Single Digital Market in Science, Education and Security" of the Scientific Research Center, NIS-3317 and National roadmaps for research infrastructures (RIs) grant number [NIS-3318]. The authors are thankful for the support through Project BG05M2OP001-1.001-0004-C01/28.02.2018 (2018-2023) Generalitat de Catalunya (grant 2017SGR1033), and the Spanish Structures of Excellence Maria de Maeztu Program through grant MDM-2017-0767 is fully acknowledged.

■ REFERENCES

- (1) Cotton, F.; Wilkinson, G.; Murillo, C.; Bochmann, M. *Advanced Inorganic Chemistry*; Wiley: New York 1988, 6.
- (2) Baran, E. J.; Monje, P. V. Oxalate biominerals. *Met. Ions Life Sci.* **2008**, *4*, 219–254.
- (3) Franceschi, V. R.; Horner, H. T. Calcium oxalate crystals in plants. *Bot. Rev.* **1980**, *46*, 361–427.
- (4) Libert, B.; Franceschi, V. R. Oxalate in crop plants. *J. Agric. Food Chem.* **1987**, *35*, 926–938.
- (5) Yeoh, J. S.; Armer, C. F.; Lowe, A. Transition metal oxalates as energy storage materials. A review. *Mater. Today Energy* **2018**, *9*, 198–222.
- (6) Pezerat, H.; Dubernat, J.; Lagier, J. Structure des oxalates dihydrates de magnésium, manganèse, fer, cobalt, nickel et zinc, existence de fautes d'empilement. *C. r. Acad. Sci. C* **1968**, *222*, 1357–1360.
- (7) Lethbridge, Z. A. D.; Congreve, A. F.; Esslemont, E.; Slawin, A. M. Z.; Lightfoot, P. Synthesis and structure of three manganese oxalates: $\text{MnC}_2\text{O}_4 \cdot 2\text{H}_2\text{O}$, $[\text{C}_4\text{H}_8(\text{NH}_2)_2][\text{Mn}_2(\text{C}_2\text{O}_4)_3]$ and $\text{Mn}_2(\text{C}_2\text{O}_4)(\text{OH})_2$. *J. Solid State Chem.* **2003**, *172*, 212–218.

- (8) Fu, X.; Wang, C.; Li, M. catena-Poly [[[diaquamanganese (II)]- μ -oxalato] monohydrate]. *Acta Crystallogr., Sect. E: Struct. Rep. Online* **2005**, *61*, m1348–m1349.
- (9) Huizing, A.; Van Hal, H. A. M.; Kwestroo, W.; Langereis, C.; Van Loosdregt, P. C. Hydrates of manganese (II) oxalate. *Mater. Res. Bull.* **1977**, *12*, 605–611.
- (10) Mancilla, N.; Caliva, V.; D'Antonio, M. C.; González-Baró, A. C.; Baran, E. J. Vibrational spectroscopic investigation of the hydrates of manganese (II) oxalate. *J. Raman Spectrosc.* **2009**, *40*, 915–920.
- (11) Nedyalkova, M.; Antonov, V. Manganese oxalates-structure-based Insights. *Open Chem.* **2018**, *16*, 1176–1183.
- (12) Hristov, H.; Nedyalkova, M.; Madurga, S.; Simeonov, V. Boron oxide glasses and nanocomposites: synthetic, structural and statistical approach. *J. Mater. Sci. Technol.* **2017**, *33*, 535–540.
- (13) Antonov, V.; Nedyalkova, M.; Tzvetkova, P.; Ahmedova, A. Solid State Structure Prediction Through DFT Calculations and ¹³C NMR Measurements: Case Study of Spiro2, 4-dithiohydantoins. *Z. Phys. Chem.* **2016**, *230*, 909–930.
- (14) Rueda, A.; Seiquer, L.; Olalla, M.; Giménez, R.; Lara, L.; Cabrera-Vique, C. Characterization of fatty acid profile of argan oil and other edible vegetable oils by gas chromatography and discriminant analysis. *J. Chem.* **2014**, *2014*, 1.
- (15) Nunes, K. P.; Toyota, R. G.; Oliveira, P. M. S.; Neves, E. G.; Soares, E. A. A.; Munita, C. S. Preliminary compositional evidence of provenance of ceramics from Hatahara archaeological site, central Amazonia. *J. Chem.* **2013**, *2013*, 1.
- (16) Al-Farraj, A. S.; Al-Wabel, M. I.; El-Saeid, M. H.; El-Naggar, A. H.; Ahmed, Z. Evaluation of groundwater for arsenic contamination using hydrogeochemical properties and multivariate statistical methods in Saudi Arabia. *J. Chem.* **2012**, *2013*, 812365.
- (17) Muilwijk, M.; Heenan, S.; Koot, A.; Van Ruth, S. M. Impact of production location, production system, and variety on the volatile organic compounds fingerprints and sensory characteristics of tomatoes. *Journal of Chemistry* **2015**, *2015*, 1.
- (18) Nedyalkova, M. A.; Donkova, B. V.; Simeonov, V. D. Chemometrics expertise in the links between ecotoxicity and physicochemical features of silver nanoparticles: environmental aspects. *J. AOAC Int.* **2017**, *100*, 359–364.
- (19) Hohenberg, P.; Kohn, W. Inhomogeneous electron gas. *Phys. Rev.* **1964**, *136*, B864.
- (20) Kohn, W.; Sham, L. J. Self-consistent equations including exchange and correlation effects. *Phys. Rev.* **1965**, *140*, A1133.
- (21) Parr, R. G. *Horizons of Quantum Chemistry*; Springer, 1980; pp 5–15.
- (22) Świdorski, G.; Kalinowska, M.; Świslocka, R.; Wojtulewski, S.; Lewandowski, W. Spectroscopic (FT-IR, FT-Raman and ¹H and ¹³C NMR) and theoretical in MP2/6-311++ G (d, p) and B3LYP/6-311++ G (d, p) levels study of benzenesulfonic acid and alkali metal benzenesulfonates. *Spectrochim. Acta, Part A* **2013**, *100*, 41–50.
- (23) Watanabe, H.; Hayazawa, N.; Inouye, Y.; Kawata, S. DFT vibrational calculations of rhodamine 6G adsorbed on silver: analysis of tip-enhanced Raman spectroscopy. *J. Phys. Chem. B* **2005**, *109*, 5012–5020.
- (24) Świdorski, G.; Wilczewska, A. Z.; Świslocka, R.; Markiewicz, K. H.; Lewandowski, W. Thermal and spectroscopic study of zinc, manganese, copper, cobalt and nickel 2, 3-pyrazinedicarboxylate. *Polyhedron* **2019**, *162*, 293–302.
- (25) Andersson, M. P.; Uvdal, P. New scale factors for harmonic vibrational frequencies using the B3LYP density functional method with the triple- ζ basis set 6-311+ G (d, p). *J. Phys. Chem. A* **2005**, *109*, 2937–2941.
- (26) Frisch, M.; Trucks, G.; Schlegel, H. B.; Scuseria, G. E.; Robb, M. A.; Cheeseman, J. R.; Scalmani, G.; Barone, V.; Mennucci, B.; Petersson, G. *Gaussian 09*; revision a. 02, Gaussian, Inc.: Wallingford, CT 2009, 200.
- (27) Giannozzi, P.; Baroni, S.; Bonini, N.; Calandra, M.; Car, R.; Cavazzoni, C.; Ceresoli, D.; Chiarotti, G. L.; Cococcioni, M.; Dabo, I. QUANTUM ESPRESSO: a modular and open-source software project for quantum simulations of materials. *J. Phys.: Condens. Matter* **2009**, *21*, 395502.
- (28) Monkhorst, H. J.; Pack, J. D. Special points for Brillouin-zone integrations. *Phys. Rev. B* **1976**, *13*, 5188.
- (29) Feynman, R. P. Forces in molecules. *Phys. Rev.* **1939**, *56*, 340.
- (30) Massart, D. L.; Kaufman, L. *The interpretation of analytical chemical data by the use of cluster analysis*; Wiley, 1983.
- (31) Vandeginste, B.; Massart, D.; De Jong, S.; Massart, D.; Buydens, L. *Handbook of chemometrics and qualimetrics: Part B*; Data handling in science and technology, Elsevier, 1998, 20.